Latin American Journal of Solids and Structures
www.lajss.org

Generalization of Carre algorithm

Abstract

The present work offers new algorithms for phase evaluation in measurements. Several phase-shifting algorithms with an arbitrary but constant phase-shift between captured intensity signs are proposed. The algorithms are similarly derived as the so called Carre algorithm. The idea is to develop a generalization of Carre algorithm that is not restricted to four images. Errors and random noise in the images cannot be eliminated, but the uncertainty due to its effects can be reduced by increasing the number of observations. The advantages of the proposed algorithm are its precision in the measures taken and immunity to noise in signs and images.

Keywords

phase shifting technique, Carre algorithm, phase calculation algorithms, measurement.

Pedro Americo Almeida Magalhaes Junior[a], Perrin Smith Neto[a] and Clovis Sperb de Barcellos[b,*]

[a]Pontificia Universidade Catolica de Minas Gerais - Av. Dom Jose Gaspar 500, 30535-610, Belo Horizonte – Minas Gerais, Brazil
[b]Universidade Federal de Santa Catarina, Florianopolis – Santa Catarina, Brazil

Received 24 Apr 2009;
In revised form 20 Aug 2009

* Author email: clovis@grante.ufsc.br

1 INTRODUCTION

Phase shifting is an important technique in engineering [2, 9, 12]. Conventional phase shifting algorithms require phase shift amounts to be known; however, errors on phase shifts are common for the phase shift modulators in real applications, and such errors can further cause substantial errors on the determinations of phase distributions. There are many potential error sources, which may affect the accuracy of the practical measurement, e.g. the phase shifting errors, detector nonlinearities, quantization errors, source stability, vibrations and air turbulence, and so on [10].

Currently, the phase shifting technique is the most widely used technique for evaluation of interference fields in many areas of science and engineering. The principle of the method is based on the evaluation of the phase values from several phase modulated measurements of the intensity of the interference field. It is necessary to carry out at least three phase shifted intensity measurements in order to determine unambiguously and very accurately the phase at every point of the detector plane. The phase shifting technique offers fully automatic calculation of the phase difference between two coherent wave fields that interfere in the process. There are various phase shifting algorithms for phase calculation that differ on the number of phase steps, on phase shift values between captured intensity frames, and on their sensitivity to the influencing factors during practical measurements [11].

2 THEORY OF PHASE SHIFTING TECHNIQUE

The fringe pattern is assumed to be a sinusoidal function and it is represented by intensity distribution I(x,y). This function can be written in general form as:

$$I(x,y) = I_m(x,y) + I_a(x,y)\cos[\phi(x,y) + \delta] \tag{1}$$

where, Im is the background intensity variation, Ia is the modulation strength, ϕ(x,y) is the phase at origin and δ is the phase shift related to the origin [3].

The general theory of synchronous detection can be applied to discrete sampling procedure, with only a few sample points. There must be at least four signal measurements needed to determine the phase ϕ and the term δ. Phase Shifting is the preferred technique whenever the external turbulence and mechanical conditions of the images remain constant over the time required to obtain the four phase-shifted frames. Typically, the technique used in this experiment is called Carre method [8]. By solving the Eq. (1) above, the phase ϕ can be determined. The intensity distribution of fringe pattern in a pixel may be represented by gray level, which varies from 0 to 255. With Carre method, the phase shift (δ) amount is treated as an unknown value. The method uses four phase-shifted images as

$$\begin{cases} I_1(x,y) = I_m(x,y) + I_a(x,y)\cos\left[\phi(x,y) - 3\delta/2\right] \\ I_2(x,y) = I_m(x,y) + I_a(x,y)\cos\left[\phi(x,y) - \delta/2\right] \\ I_3(x,y) = I_m(x,y) + I_a(x,y)\cos\left[\phi(x,y) + \delta/2\right] \\ I_4(x,y) = I_m(x,y) + I_a(x,y)\cos\left[\phi(x,y) + 3\delta/2\right] \end{cases} \tag{2}$$

Assuming the phase shift is linear and does not change during the measurements, the phase at each point is determined as

$$\phi = \arctan\left\{\frac{\sqrt{\left[(I_1 - I_4) + (I_2 - I_3)\right]\ \left[3(I_2 - I_3) - (I_1 - I_4)\right]}}{(I_2 + I_3) - (I_1 + I_4)}\right\} \tag{3}$$

Expanding Eq. (3), we obtain the Carre method as:

$$\tan(\phi) = \frac{\sqrt{\begin{vmatrix} -I_1^2 & +2I_1I_2 & -2I_1I_3 & +2I_1I_4 \\ & +3I_2^2 & -6I_2I_3 & -2I_2I_4 \\ & & +3I_3^2 & +2I_3I_4 \\ & & & -I_4^2 \end{vmatrix}}}{|-I_1 + I_2 + I_3 - I_4|} \tag{4}$$

or emphasizing only the matrix of coefficients of the numerator and the denominator:

$$\tan(\phi) = \frac{\sqrt{|Num|}}{|Dem|} \qquad Num = \begin{bmatrix} -1 & 2 & -2 & 2 \\ & 3 & -6 & -2 \\ & & 3 & 2 \\ & & & -1 \end{bmatrix} \quad Dem = \begin{bmatrix} -1 & 1 & 1 & -1 \end{bmatrix} \tag{5}$$

Almost all the existing phase-shifting algorithms are based on the assumption that the phase-shift at all pixels of the intensity frame is equal and known. However, it may be very difficult to achieve this in practice. Phase measuring algorithms are more or less sensitive to some types of errors that can occur during measurements with images. The phase-shift value is assumed unknown but constant in phase calculation algorithms, which are derived in this article. Consider now the constant but unknown phase shift value δ between recorded images of the intensity of the observed interference field.

Considering N phase shifted intensity measurements, we can write for the intensity distribution Ik at every point of k recorded phase shifted interference patterns.

$$I_k(x,y) = I_m(x,y) + I_a(x,y)\cos\left[\phi(x,y) + \left(\frac{2k-N-1}{2}\right)\delta\right] \tag{6}$$

where k = 1,..,N and N being the number of frames.

In Novak [10], several five-step phase-shifting algorithms insensitive to phase shift calibration are described, and a complex error analysis of these phase calculation algorithms is performed. The best five-step algorithm, Eq. (7), seems to be a very accurate and stable phase shifting algorithm with the unknown phase step for a wide range of phase step values.

$$\begin{cases} a_{jk} = I_j - I_k \\ b_{jk} = I_j + I_k \end{cases} \qquad \tan(\phi) = \frac{\sqrt{4a_{24}^2 - a_{15}^2}}{2I_3 - b_{15}} = \frac{\sqrt{4(I_2-I_4)^2-(I_1-I_5)^2}}{2I_3-I_1-I_5} \tag{7}$$

Expanding Eq. (7), we obtain the Novak method as:

$$\tan(\phi) = \frac{\sqrt{\begin{vmatrix} -I_1^2 & & & & +2I_1I_5 \\ & +4I_2^2 & -8I_2I_4 & & \\ & & +4I_4^2 & & \\ & & & -I_5^2 & \end{vmatrix}}}{|-I_1 + 2I_3 - I_5|} \tag{8}$$

or emphasizing only the matrix of coefficients of the numerator and the denominator:

$$\tan(\phi) = \frac{\sqrt{|Num|}}{|Dem|} \qquad Num = \begin{bmatrix} -1 & 0 & 0 & 0 & 2 \\ & 4 & 0 & -8 & 0 \\ & & 0 & 0 & 0 \\ & & & 4 & 0 \\ & & & & -1 \end{bmatrix} \quad Dem = \begin{bmatrix} -1 & 0 & 2 & 0 & -1 \end{bmatrix} \tag{9}$$

3 PROPOSED ALGORITHMS

It is presently proposed a general algorithm for calculating the phase for any number, N, of images tan (ϕ) = Sqrt (Abs (Num)) / Abs (Dem) where:

$$\tan(\phi) = \frac{\sqrt{|Num|}}{|Dem|} = \frac{\sqrt{\left|\sum_{r=1}^{N}\sum_{s=r}^{N} n_{rs} I_r I_s\right|}}{\left|\sum_{r=1}^{N} d_r I_r\right|} \tag{10}$$

or expanding the summations and allowing an arbitrary number of lines

$$\tan(\phi) == \frac{\sqrt{\left|\begin{array}{cccccc} n_{1,1}I_1^2 & +n_{1,2}I_1I_2 & +n_{1,3}I_1I_3 & +n_{1,4}I_1I_4 & ... & +n_{1,N}I_1I_N \\ & +n_{2,2}I_2^2 & +n_{2,3}I_2I_3 & +n_{2,4}I_2I_4 & ... & +n_{2,N}I_2I_N \\ & & +n_{3,3}I_3^2 & +n_{3,4}I_3I_4 & ... & +n_{3,N}I_3I_N \\ & & & +n_{4,4}I_4^2 & ... & +n_{4,N}I_4I_N \\ & & & & ... & ... \\ & & & & & +n_{N,N}I_N^2 \end{array}\right|}}{|d_1I_1 + d_2I_2 + d_3I_3 + d_4I_4 + ... + d_{N-1}I_{N-1} + d_NI_N|} \tag{11}$$

or emphasizing only the matrix of coefficients of the numerator and the denominator:

$$\tan(\phi) = \frac{\sqrt{|Num|}}{|Dem|} \quad \begin{cases} Num = \begin{bmatrix} n_{1,1} & n_{1,2} & n_{1,3} & n_{1,4} & ... & n_{1,N} \\ & n_{2,2} & n_{2,3} & n_{2,4} & ... & n_{2,N} \\ & & n_{3,3} & n_{3,4} & ... & n_{3,N} \\ & & & n_{4,4} & ... & n_{4,N} \\ & & & & ... & ... \\ & & & & & n_{N,N} \end{bmatrix} \\ Dem = \begin{bmatrix} d_1 & d_2 & d_3 & d_4 & ... & d_{N-1} & d_N \end{bmatrix} \end{cases} \tag{12}$$

To display of the phase calculation algorithm in this way permits the viewing of symmetries and plans of sparse matrix. The use of the absolute value in the numerator and in the denominator restricts the angle between 0 and 90 degree but avoids negative roots, and, in addition, eliminates false angles to be found. Subsequent considerations will later remove this restriction [3, 10, 11].

In the tested practical applications, it was noticed an increase of 20% in the processing time when using 16 images instead of 4 when processing the standard Carre algorithm, due to many zero coefficients. But if one changes the coefficients from integer type to real, the processing time for the evaluation of phase practically duplicates because real numbers use more memory and more processing time to evaluate floating point additions and multiplications, which are many in the algorithms with large quantity of images.

The shift on the problem focus of obtaining algorithms for calculating the phase of an analytical problem of a numerical vision is a great innovation and breaks a paradigm that was hitherto used by several authors. After several attempts in numerical modeling the problem, the following mathematical problem was identified (13):

$$
Minimal \quad \sum_{r=1}^{N}\sum_{s=r}^{N}|n_{r,s}| + \sum_{r=1}^{N}|d_r|
$$

$$
subject \quad \begin{cases}
i) & \tan(\phi) = \mathrm{Sqrt}(|\mathrm{Num}|)/|\mathrm{Dem}| & \text{number of variables} \\
 & \tan^2(\phi^v)\left(\sum_{r=1}^{N} d_r I_r^v\right)^2 = \sum_{r=1}^{N}\sum_{s=r}^{N} n_{r,s} I_r^v I_s^v, & v = 1..\left[\frac{(N+1)N}{2} + N\right] \\
ii) & \sum_{s=r}^{N}|n_{r,s}| + |d_r| \geq 1, & r = 1..N, \text{enter all frames} \\
 & \sum_{s=r}^{N}|n_{s,r}| + |d_r| \geq 1, & r = 1..N, \text{enter all frames} \\
iii) & -2N \leq n_{r,s} \leq 2N, & r = 1..N, s = r..N \\
iv) & -2N \leq d_s \leq 2N, & r = 1..N \\
v) & n_{r,s} \text{ are integer}, & r = 1..N, s = r..N \\
vi) & d_r \text{ are integer}, & r = 1..N \\
vii) &
\end{cases}
$$

where for each v:

$$
\begin{cases}
I_k^v(x,y) = I_m^v(x,y) + I_a^v(x,y)\cos\left[\phi^v(x,y) + \left(\frac{2k-N-1}{2}\right)\delta^v\right] & , k = 1..N \\
I_m^v \in [0;\ 128] \quad random \quad and \quad real \\
I_a^v \in [0;\ 127] \quad random \quad and \quad real \\
\phi^v \in [-\pi;\ \pi] \quad random \quad and \quad real \\
\delta^v \in [-2\pi;\ 2\pi] \quad random \quad and \quad real
\end{cases}
\tag{13}
$$

The coefficients of matrices of the numerator (nrs) and denominator (dr) must be integer in order to increase the performance of computer algorithm, as the values of the intensity of the images (Ik) are also integers ranging from 0 to 255. Modern computers perform integer computations (additions and multiplications) much faster than floating point ones. It should be noted that currently the commercial digital photographic cameras already present graphics resolution above 12 Mega pixels and that the evaluation of phase (ϕ) should be done pixel to pixel. Another motivation is the use of memory: integer values can be stored on a single byte while real values use, at least, 4 bytes. The present scheme only uses real numbers in the square root of the numerator, the division by denominator, and the arc-tangent over the entire operation.

The idea of obtaining a minimum sum of the values of absolute or module of the coefficients of matrices of the numerator (nrs) and denominator (dr) comes from the attempt to force these factors to zero, for computational speed up and for reducing the required memory, since zero terms in sparse matrices do not need to be stored. It is also important that those ratios are not very large so that the values of the sum of the numerator and of the denominator do not have very high value in order fit into an integer variable. For a precise phase evaluation, these factors will increase the values of the intensity of the images (Ik) that contains errors due to noise in the image, in its discretization in pixels and in shades of gray.

The first restriction of the problem (13) is the Eq. (10) which is squared to form of the relation that one is seeking. Note that the results of solving the mathematical problem of the coefficients are matrices on the numerator (nrs) and denominator (dr), so the number of unknowns is given by ν. To ensure that one has a hyper-restricted problem, the number of

restrictions must be greater or at least equal to the number of variables. The ν restrictions of the model are obtained through random choice of values for Im, Ia, ϕ and δ and using the Eq. (6) to compute Ik. Tests showed that for even low numbers for other values of ν, the mathematical problem leads only to one optimal solution, while it becomes more time consuming. Indeed the values of Im, Ia, ϕ and δ can be any real number, but to maintain compatibility with the problem images, it was decided to limit Im from 0 to 128 and Ia between 0 and 127 so that Ik be between 0 and 255.

The restrictions *ii* and *iii* of the problem are based on the idea that all image luminous intensities, Ik, must be present in the algorithm. It increases the amounts of samples to reduce the noise of random images. This requires that all of sampling images enter the algorithm for phase calculation. This is achieved by imposing that the sum of the absolute values of the coefficients of each row or column of the matrix of each of the numerator (nrs), plus the module at the rate corresponding to that image in the denominator (dr) is greater than or equal to 1. Thus the coefficients on algorithm to calculate the phase for a given image Ik will not be all zeros, ensuring their participation in the algorithm.

Restrictions *iv* and *v* of the problem are used to accelerate the solution of this mathematical model. This limitation in the value of the coefficients of matrices of the numerator (nrs) and denominator (dr) presents a significant reduction in the universe of search and in the search of a solution of the model optimization. Whenever N is greater than 16, the coefficients of matrices of the numerator (nrs) and denominator (dr) can be limited to the interval [-4. 4]. The search is restricted to coefficients of matrices of the numerator (nrs) and denominator (dr) which are integers, of small value, and meeting the restrictions of the model, it does not need to be minimized (desirable but not necessary).

Once a solution to the problem is found, it can become a restriction. Therefore, solving the problem again leads to a new different solution. This allows the problem (13) to lead to many different algorithms for a given value of N, making it very flexible and the numerical problem comprehensive. The following multi-step algorithms for phase calculation uses well known trigonometric relations and branch-and-bound algorithm [6] for pure integer nonlinear programming with the mathematic problem (13). Next, tables show some algorithms.

Table 1 Matrix of Coefficient for N = 4 and N=5, with type $tan(\phi) = Sqrt(|Num|)/|Dem|$.

N = 4	Num	-1	2	-2	2	
			3	-6	-2	
		a)		3	2	
					-1	
	Dem	-1	1	1	-1	
N = 5	Num	-1	0	0	0	2
			4	0	-8	0
		a)		0	0	0
					4	0
						-1
	Dem	-1	0	2	0	-1

Following the model presented of uncertainty analysis in [1, 10], these new algorithms have

Table 2 Matrix of Coefficient for N = 6,...,12, with type $tan(\phi) = Sqrt(|Num|)/|Dem|$.

N = 6	Num	-1	0	-1	1	0	2		-1	0	0	0	0	2		-1	0	-2	2	0	2		-1	2	-2	2	-2	2		-1	2	0	0	0	-2	2
			3		0		1			2	-2	-2	0	0			4	0	0	-1	0	2			1	-2	2	-2	2			1	0	4	0	0	2	0
		a)		-1		0	1	-1	b)	1	1	2	0	0	c)		0	2	2	-1	0	2	-2	d)		2	-4	2	-1	1	e)		0	4	-8	0	0	-1
				0		0	3	-1					-1	-1							0	-1															-1
	Dem	-1	0	1	1	0	-1		-1	0	1	1	0	-1		-1	0	1	1	0	-1		-1	1	0	0	1	1		-1	1	0	0	1	-1	-1

N = 7	Num	-1	-2	-3	0	3	2	2		-1	2	-5	0	5	-2	2			-1	-2	1	0	0	-1	2	0	0	0	2	2
			4	6	0	-6	-8	3			6	-6	0	0	-12	5				0		6	0	-6			1	6	5	0	-6	-2	0	0	0	0
		a)		2	0	-4	-6	0	b)			0	0	0	6	0	c)				0		0	-6	0	1	d)			0	-10	-6	0	0	-2
					0	0	0	-3							0	-5							0	0	-2					0	5	1	0	0	-1
	Dem	-1	-1	1	2	1	-1	-1		-1	1	1	-2	-2	1	-1			-1	-1	1	2	1	-1	-1	-1	-1	-1	1	2	1	-1	-1	-1	-1	-1

N = 8	Num	-1	0	1	0	0	-1	0	2			-1	0	0	0	1	0	0	0	2			-1	0	0	1	1	-1	0	0	0	0	0	0	0	0	2	0
			1	0	2	2	0	-2	0			2	0	0	1	1	0	0	0	0			0	0	0	3	0	0	0	0	0	0	0	0	0	0	0	0	0
		a)		1	1	1	-2	1	0			b)		1	-1	-2	1	0	0	0			c)		3	0	0	0	0	0	1	0	0	0	1	0	0	0	0
							1	0	-1							1	0	0	0	-1																			-1
	Dem	-1	0	1	0	0	1	0	-1			-1	0	1	0	0	1	0	0	-1			-1	0	0	1	1	0	0	0	1	0	0	0	1	0	0	0	-1

N = 9	Num	-1	2	-1	0	0	0	1	-2	2		-1	2	-1	1	0	-1	1	-2	2			-1	-2	-2	0	0	0	2	2	2	2
			0	-2	0	0	0	2	0	1			0	-3	1	0	0	0	-1	3	0	-1		1	-2	6	-2	-8	-2	-2	2	0	0
		a)		6	0	-6	0	-12	0	0	0	b)		5	-5	1	5	0	-2	-10	5	0	c)		4	1	0	0	6	-6	0	6	0	0
					0	0	0	6	0	0	0			0	1	0	0	1	0	5	-5	3					1	0	1	4	1	0	1	0	-2	-2
	Dem	-1	1	0	-1	2	-1	0	1	-1	0	-1	1	0	-1	2	-1	0	1	-1	5	1	-1	-1	-1	0	1	2	1	0	-1	-1	-1	-1	-1	-1

N = 10	Num	-1	0	1	0	0	0	0	0	-1	0	2	0		-1	0	-1	0	1	0	0	0	-1	0	2			-1	0	0	0	0	0	0	0	0	2	0
			0	0	0	-1	1	0	0	-2	0	-1	0			1	0	1	1	0	0	-1	-1	-2	0	1	0	0	2	0	0	0	0	-1	0	0	0	0	0
		a)		0	1	1	-1	-2	1	0	0	1	0	0	b)		1	1	1	0	0	0	-2	-1	-1	0	0	0	c)										
										1	0	0	0										0	1	0	0	0	0	0	0	0	0	0	0	0	0	0	0
	Dem	-1	0	1	0	0	0	0	1	0	0	-1	0		-1	0	0	0	1	1	0	0	0	0	1	0	1	0	0	0	0	1	0	0	0	0	0	-1

N = 11	Num	-1	0	-1	-2	0	0	0	2	0	1	0	0	2		-1	0	-1	-1	0	0	0	0	1	1	0	2		-1	-2	0	0	0	0	0	2	2	2
			1	0	2	0	0	0	0	-2	0	-4	-2	0			1	0	2	0	0	0	0	0	-1	1	0			1	0	2	2	0	0	0	-2	-2	-2
		a)		1	1	1	0	0	0	-2	0	0	0	0	b)		0	0	3	1	0	0	0	-4	0	0	-1	0	c)		1	-4	-3	0	0	0	2	-4	0
							0	0	-4	0	0	0	2	0			0	0	1	0	0	0	0	2	0	0	1	0			0	0	3	2	0	0	0	2	-2	2
	Dem	-1	0	0	-1	1	2	1	-1	0	0	1	0	-1		-1	0	0	-1	1	2	1	-1	0	0	0	-1	-1		-1	-1	1	0	0	2	0	0	1	-1	-1

N = 12	Num	-1	0	1	0	0	0	0	0	0	0	-1	0	2		-1	0	1	0	0	0	0	0	0	0	0	1	0	2	0
			1	0	0	-1	0	0	0	1	0	0	0	-1			1	0	0	0	0	0	0	0	0	1	0	0	0	-1
		a)				0	0	0	1	1	0	-2	0	0	b)		0	0	0	0	0	-1	-1	-2	-1	1	0	0	0	0
						1					-1	0	1	0																
	Dem	-1	0	1	0	0	0	0	0	0	1	0	-1	0		-1	0	1	0	0	0	0	0	0	1	0	0	0	-1	-1

Table 3 Matrix of Coefficient for N = 13,...,16, with type $tan(\phi) = Sqrt(|Num|)/|Dem|$.

N = 13	Num	-1	2	-1	0	0	0	0	0	0	0	1	-2	2
			0	-2	0	-2	0	0	0	2	0	2	0	-2
				2	2	1	-2	0	2	-1	-2	-4	2	1
		a)			2	-2	-1	0	1	2	-4	-2	0	0
						1	-2	0	2	-2	2	-1	2	0
							1	0	-2	2	1	2	0	0
								0	0	0	0	0	0	0
									1	-2	-1	-2	0	0
										1	-2	1	-2	0
											2	2	0	0
												2	-2	-1
													0	2
														-1
	Dem	-1	1	0	-1	0	0	2	0	0	-1	0	1	-1

N = 13	Num	-1	2	-2	-2	0	1	0	-1	0	2	2	-2	2
			1	0	0	-1	1	0	-1	1	0	0	-2	-2
				2	0	0	-1	0	1	0	0	-4	0	2
		b)			2	-2	-1	0	1	2	-4	0	0	2
						2	-2	0	2	-4	2	0	1	0
							-1	0	2	2	1	1	-1	-1
								0	0	0	0	0	0	0
									-1	-2	-1	-1	1	1
										2	-2	0	-1	0
											2	0	0	-2
												2	0	-2
													1	2
														-1
	Dem	-1	1	0	-1	0	0	2	0	0	-1	0	1	-1

N = 14	Num	-1	0	1	0	0	0	0	0	0	0	0	-1	0	2
			1	0	-1	0	0	0	0	0	0	1	0	-2	0
				0	0	1	0	0	0	0	-1	0	0	0	-1
		a)			-1	0	-1	0	0	1	0	2	0	1	0
						1	0	-1	1	0	-2	0	-1	0	0
							1	1	-1	-2	0	1	0	0	0
								1	-2	-1	1	0	0	0	0
									1	1	-1	0	0	0	0
										1	0	-1	0	0	0
											1	0	1	0	0
												-1	0	-1	0
													0	0	1
														1	0
															-1
	Dem	-1	0	1	0	0	0	0	0	0	0	0	1	0	-1

N = 14	Num	-1	0	-1	0	0	0	0	0	0	0	0	1	0	2
			1	0	1	0	0	0	0	0	0	-1	0	-2	0
				1	0	0	0	0	0	0	0	0	-2	0	1
		b)			0	0	-1	0	0	1	0	0	0	-1	0
						0	2	0	0	-2	0	0	0	0	0
							0	-1	1	0	-2	1	0	0	0
								1	-2	1	0	0	0	0	0
									1	-1	0	0	0	0	0
										0	2	-1	0	0	0
											0	0	0	0	0
												0	0	1	0
													1	0	-1
														1	0
															-1
	Dem	-1	0	0	0	1	0	0	0	0	1	0	0	0	-1

N = 15	Num	-1	-2	0	1	0	0	0	0	0	0	0	-1	0	2	2
			1	1	-1	0	0	0	0	0	0	0	1	-1	-2	2
				0	0	-1	2	0	0	0	-2	1	0	0	-1	0
		a)			1	2	2	-2	0	2	-2	-2	-2	0	1	-1
						2	-2	0	0	0	2	-4	-2	1	0	0
							0	1	0	-1	0	2	-2	-2	0	0
								2	0	-4	-1	0	2	0	0	0
									0	0	0	0	0	0	0	0
										2	1	0	-2	0	0	0
											0	-2	2	2	0	0
												2	2	-1	0	0
													1	0	-1	1
														0	1	0
															1	-2
																-1
	Dem	-1	-1	1	0	0	0	0	2	0	0	0	0	1	-1	-1

N = 16	Num	-1	0	1	0	0	0	0	0	0	0	0	0	0	-1	0	2
			1	0	-1	0	0	0	0	0	0	0	0	1	0	-2	0
				0	0	1	0	0	0	0	0	0	-1	0	0	0	-1
		a)			-1	0	0	0	0	0	0	0	0	2	0	1	0
						0	0	-1	0	0	1	0	0	0	-1	0	0
							1	0	-1	1	0	-2	0	0	0	0	0
								1	1	-1	-2	0	1	0	0	0	0
									1	-2	-1	1	0	0	0	0	0
										1	1	-1	0	0	0	0	0
											1	0	-1	0	0	0	0
												1	0	0	0	0	0
													0	0	1	0	0
														-1	0	-1	0
															0	0	1
																1	0
																	-1
	Dem	-1	0	1	0	0	0	0	0	0	0	0	0	0	1	0	-1

excellent results with the application of Monte Carlo-based technique of uncertainty propagation. The Monte Carlo-based technique requires first assigning probability density functions (PDFs) to each input quantity. A computer algorithm is set up to generate an input vector P = (p1. . . pn)T; each element pj of this vector is generated according to the specific PDF assigned to the corresponding quantity pj. By applying the generated vector P to the model Q = M(P), the corresponding output value Q can be computed. If the simulating process is repeated n times (n >> 1), the outcome is a series of indications (q1. . . qn) whose frequency distribution allows us to identify the PDF of Q. Then, irrespective of the form of this PDF, the estimate qe and its associated standard uncertainty u(qe) can be calculated by

$$q_e = \frac{1}{n}\sum_{l=1}^{n} q_l, \qquad (14)$$

and

$$u(q_e) = \sqrt{\frac{1}{(n-1)}\sum_{l=1}^{n}(q_l - q_e)^2}. \tag{15}$$

The influence of the error sources affecting the phase values is considered in these models through the values of the intensity Ik. This is done by modifying Eq. (6):

$$I_k(x,y) = I_m(x,y) + I_a(x,y)\cos\left[\phi(x,y) + \left(\frac{2k-N-1}{2}\right)(\delta+\theta) + \varepsilon_k\right] + \xi_k. \tag{16}$$

Comparing Eqs. (6) and (16), it can be observed that 3 input quantities, (θ, ϵk, ξk), were included. θ allows us to consider in the uncertainty propagation the systematic error used to induce the phase shift, is not adequately calibrated. The error bound allowed us to assign to θ a rectangular PDF over the interval (-π/10 rad, +π/10 rad). ϵk allows us to account for the influence of environmental perturbations. The error bound allowed us to assign to ϵk a rectangular PDF over the interval (-π/20 rad, +π/20 rad). ξk allows us to account for the nearly random effect of the optical noise. The rectangular PDFs assigned to ξk should be in the interval (-10, +10).

The values of ϕ were considered given in the range (0, π/2). A computer algorithm was set up to generate single values of (θ, ϵk, ξk) according to the corresponding PDFs. With the generated values of the input quantities, we evaluated the phase ϕ by using the new algorithms. Since this simulating process and the corresponding phase evaluation were repeated n = 104 = 10000 times, we were able to form the series (ϕ1...ϕ10000) with the outcomes.

The algorithms with letters (a) (Table 1, 2 and 3) are better, more accuracy, more robust and more stable for the random noise. The tests show that the optimum phase-shift interval with which the algorithm gives minimum uncertainty for the noise is near of π/2 radians (Fig. 1).

Fig. 2 shows the average of the standard uncertainty u(ϕ) generated with values ϕ in range (0, π/2) by using new algorithms. It can be observed that the uncertainty by new algorithms diminish as number of images increases.

4 BEFORE UNWRAPPING, CHANGE $\phi \in$ [0, π/2] TO ϕ * $\in$[-π, π]

Because of the character of the evaluation algorithms, only phase values $\phi \in [0, \pi/2]$ were calculated. For unequivocal determination of the wrapped phase values ϕ it was necessary to test four values ϕ, -ϕ, ϕ -π and -ϕ +π using values of Ik and small systems. With this, the value ϕ * $\in$[-π, π] was obtained [2, 3, 10, 11]. In case N=5, with $I1$, I 2, I 4 e I 5, δ was found in first equation and the values ϕ, -ϕ, ϕ-π and -ϕ+π were attributed to ϕ* in order to test the other equation and Ia was found using a second equation. As an example, for each (x, y) it was tested the four values ϕ, -ϕ, ϕ-π and -ϕ+π in (Addition and subtraction of first, last and middle frames, the Ik):

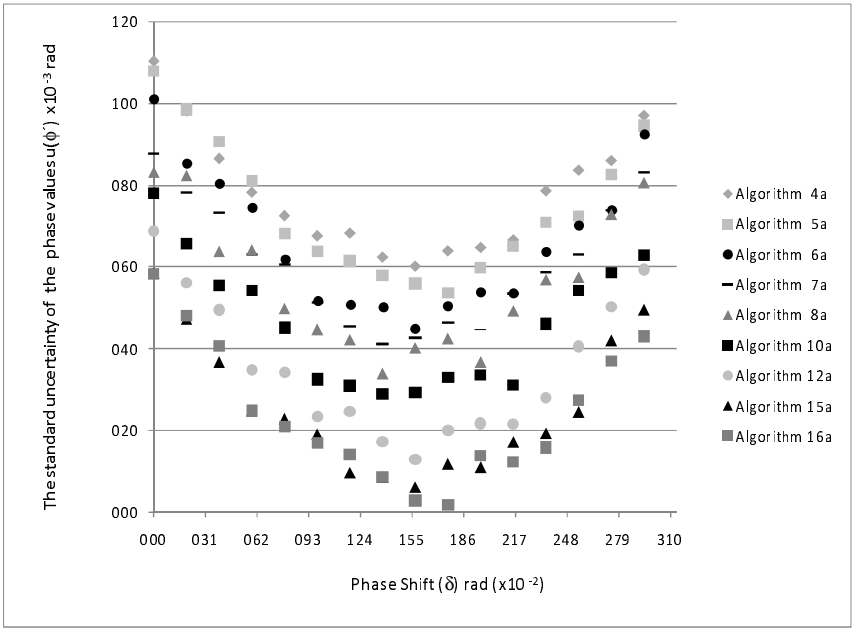

Figure 1 Standard uncertainty of the phase values u(ϕ) using new algorithms with variation of phase shift (δ). Note that the uncertainty is smaller close by $\delta=\pi/2$ and decreases with increasing the number of images.

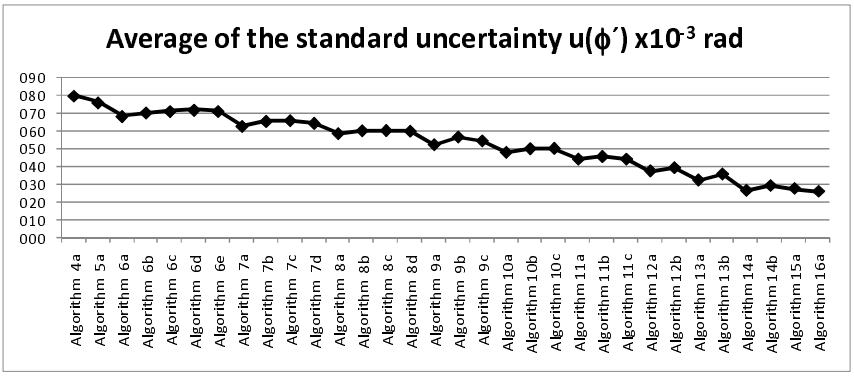

Figure 2 Average of the standard uncertainty u(ϕ) by using new algorithms. Note that the uncertainty decreases with increasing the number of images.

$$even \quad N=4\begin{cases} \cos\left(\delta/2\right) = \pm\sqrt{\frac{I_1-I_4}{4(I_2-I_3)}} \\ I_1 - I_4 = 2I_a \sin(\phi^*)\sin\left(3\delta/2\right) \\ I_2 - I_3 = 2I_a \sin(\phi^*)\sin\left(\delta/2\right) \\ (I_1+I_4)-(I_2+I_3) = 2I_a\cos(\phi^*)\left[\cos\left(3\delta/2\right)-\cos\left(\delta/2\right)\right] \\ I_1 - I_3 = I_a\left[\cos\left(\phi^* - 3\delta/2\right)-\cos\left(\phi^* + \delta/2\right)\right] \end{cases} \tag{17}$$

$$odd \quad N=5\begin{cases} \cos(\delta) = \frac{I_1-I_5}{2(I_2-I_4)} \\ I_1 - I_5 = 2I_a\sin(\phi^*)\sin(2.\delta) \\ I_2 - I_4 = 2I_a\sin(\phi^*)\sin(\delta) \\ I_1 + I_5 - 2.I_3 = 2I_a\cos(\phi^*)[\cos(2.\delta)-1] \\ I_2 + I_4 - 2.I_3 = 2I_a\cos(\phi^*)[\cos(\delta)-1] \end{cases} \tag{18}$$

In a different approach, for unambiguous determination of the wrapped phase values, it is necessary to test four values ϕ, $-\phi$, $\phi-\pi$ and $-\phi+\pi$ using values of Ik and to solve small nonlinear systems (Newton-Raphson methods). For each angle ϕ, $-\phi$, $\phi-\pi$ and $-\phi+\pi$ solve the nonlinear system by Newton-Raphson in Eq. (19), getting the values of Im, Ia and δ.

$$\begin{cases} I_1 - \left(I_m + I_a\cos\left[\phi* + \left(\frac{2.1-N-1}{2}\right)\delta\right]\right) = 0 \\ I_2 - \left(I_m + I_a\cos\left[\phi* + \left(\frac{2.2-N-1}{2}\right)\delta\right]\right) = 0 \\ I_3 - \left(I_m + I_a\cos\left[\phi* + \left(\frac{2.3-N-1}{2}\right)\delta\right]\right) = 0 \end{cases} \tag{19}$$

With the values of Im, Ia and δ, test in Eq. (20) and find the correct angle $\phi^* \in [-\pi, \pi]$.

$$\begin{cases} I_4 - \left(I_m + I_a\cos\left[\phi* + \left(\frac{2.4-N-1}{2}\right)\delta\right]\right) = 0 \\ \quad\quad\quad\quad ... \\ I_N - \left(I_m + I_a\cos\left[\phi* + \left(\frac{2N-N-1}{2}\right)\delta\right]\right) = 0 \end{cases} \tag{20}$$

5 TESTING AND ANALYSIS OF ERROR

The phase ϕ^* obtained from the Phase Shifting Algorithm above is a wrapped phase, which varies from $-\pi/2$ to $\pi/2$. The relationship between the wrapped phase and the unwrapped phase may thus be stated as:

$$\Psi(x,y) = \phi*(x,y) + 2\pi j(x,y) \tag{21}$$

where j is an integer number, ϕ^* is a wrapped phase and ψ is an unwrapped phase.

The next step is to unwrap the wrapped phase map [13]. When unwrapping, several of the phase values should be shifted by an integer multiple of 2π. Unwrapping is thus adding or subtracting 2π offsets at each discontinuity encountered in phase data. The unwrapping procedure consists in finding the correct field number for each phase measurement [4, 7, 14].

The modulation phase ψ obtained by unwrapping physically represents the fractional fringe order numbers in the Moire images. The shape can be determined by applying the out-of-plane deformation equation for Shadow Moire:

$$Z(x,y) = \frac{p\Psi(x,y)}{(\tan\alpha + \tan\beta)} \tag{22}$$

where: Z(x,y) = elevation difference between two points located at body surface to be analyzed; p = frame period; α = light angle; β = observation angle.

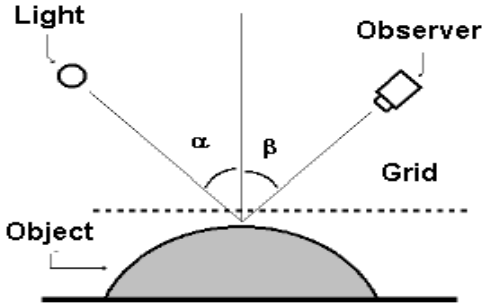

Figure 3 Layout of experiment.

Presently, the experiments were carried out using square wave grating with metricconverterProductID1 mm1 mm frame grid period, light source is common white of 300 watts without using plane waves, light angle (α) and observation angle (β) are 45 degrees, the object surface are white and smooth and the resolution of photo is one mega pixel. The phase stepping is made by displacing of the grid in the horizontal direction in fractions of millimetres (Fig. 3).

To test the new algorithms for phase calculation, they were used with the technique of Shadow Moire [5] for an object with the known dimensions and to evaluate the average error the Eq. (23). This process was started with 4 images, again with 5, then 6 and so on. The idea was to show that with the increasing number of images the average error tends to decrease. Figure 4 shows this procedure.

$$Error \quad Median \quad (E) = \frac{1}{M}\sum_{i=1}^{M} |Z_i^e - Z_i| \tag{23}$$

Where M is number *of pixels* of the image, Zie is the exact value of the size of the object being measured and Zi is value measured by the new algorithm.

To compare the new algorithms for calculating the phase, 21 sets of 16 photos each were selected. Each set was computed using the average error of 4 to 16 images and using algorithms to evaluate which the number of images was. It was estimated an average of errors, then it was 21 sets using 4 to 16 images in each set (μ4,μ5,μ6, ..., μ16). The hypothesis of testing on the difference in the means μA - μB of two normal populations is being considered at the moment. A more powerful experimental procedure is to collect the data in pairs – that is, to make two hardness readings on each specimen, one with each tip. The test procedure would then

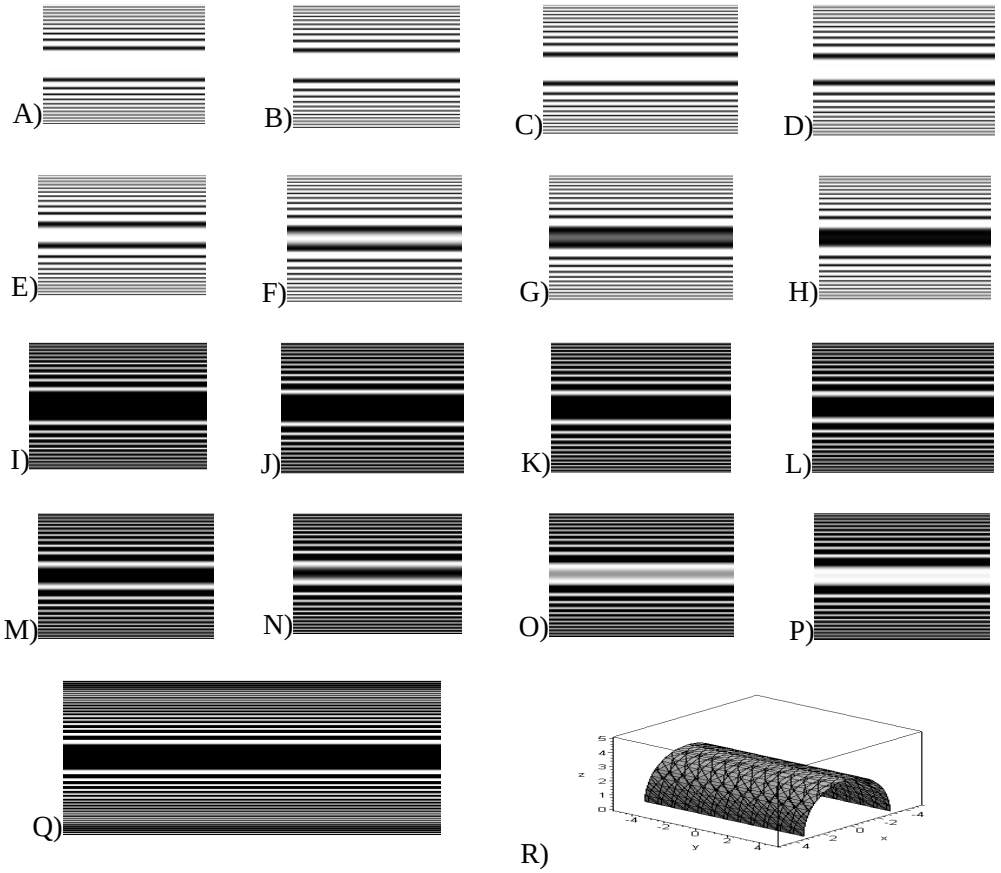

Figure 4 One set of photos of 1 Megabyte. Original Shadow Moire Images. 16-frame Phase-shifting algorithm. [A-P]. Wrapped phase[Q]. Result in 3D [R]. (Semi-cylinder of a motor with diameter of 6 cm, length of 12 cm and frame period of grid with 1 mm).

consist of analyzing the differences between hardness readings on each specimen. If there is no difference between tips, the mean of the differences should be zero. This test procedure is called the paired t-test [13]. Specifically, testing H0:μA-μB=0 against H1: μA-μB$\neq$0. Test statistics is t0=D/(SD/$\sqrt{}$21) where D is the sample average of the differences and SD is the sample standard deviation of these differences. The rejection region is t0>tα/2,20 or t0<-tα/2,20.

After doing the statistical test (H0:μA-μB=0 against H1: μA-μB$\neq$0) it was noticed that one can not reject the zero hypothesis when using different algorithms, but with the same number of images. Also, the null hypothesis can be rejected when using different algorithm with different numbers of images with level of significance (α=0.05). It was concluded that the algorithms for phase calculation with a greater number of images are more accurate than those that have a smaller number of images.

Table 4 Testing hypotheses about the difference between two means with paired t-test, H0:μA-μB=0 against H1: μA-μB≠0. The P-value is the smallest level of significance that would lead to rejection of the null hypothesis H0 with the given data.

P-Value		Number of Images and Formula																												
Number of Image and Formula		4	5	6					7				8				9			10			11			12		13		14		15
		a	a	a	b	c	d	e	a	b	c	d	a	b	c	d	a	b	c	a	b	c	a	b	c	a	b	a	b	a	b	a
4	a																															
5	a	0%																														
6	a	0%	0%																													
	b	0%	0%	65%																												
	c	0%	0%	80%	77%																											
	d	0%	0%	39%	13%	19%																										
	e	0%	0%	49%	30%	41%	71%																									
7	a	0%	0%	0%	0%	0%	0%	0%																								
	b	0%	0%	0%	0%	0%	0%	0%	67%																							
	c	0%	0%	0%	0%	0%	0%	0%	68%	96%																						
	d	0%	0%	0%	0%	0%	0%	0%	26%	67%	59%																					
8	a	0%	0%	0%	0%	0%	0%	0%	0%	0%	0%	0%																				
	b	0%	0%	0%	0%	0%	0%	0%	0%	0%	0%	0%	69%																			
	c	0%	0%	0%	0%	0%	0%	0%	0%	0%	0%	0%	65%	98%																		
	d	0%	0%	0%	0%	0%	0%	0%	0%	0%	0%	0%	75%	46%	48%																	
9	a	0%	0%	0%	0%	0%	0%	0%	0%	0%	0%	0%	0%	0%	0%	0%																
	b	0%	0%	0%	0%	0%	0%	0%	0%	0%	0%	0%	0%	0%	0%	0%	26%															
	c	0%	0%	0%	0%	0%	0%	0%	0%	0%	0%	0%	0%	0%	0%	0%	79%	22%														
10	a	0%	0%	0%	0%	0%	0%	0%	0%	0%	0%	0%	0%	0%	0%	0%	0%	0%	0%													
	b	0%	0%	0%	0%	0%	0%	0%	0%	0%	0%	0%	0%	0%	0%	0%	0%	0%	0%	71%												
	c	0%	0%	0%	0%	0%	0%	0%	0%	0%	0%	0%	0%	0%	0%	0%	0%	0%	0%	65%	84%											
11	a	0%	0%	0%	0%	0%	0%	0%	0%	0%	0%	0%	0%	0%	0%	0%	0%	0%	0%	0%	0%	0%										
	b	0%	0%	0%	0%	0%	0%	0%	0%	0%	0%	0%	0%	0%	0%	0%	0%	0%	0%	0%	0%	0%	32%									
	c	0%	0%	0%	0%	0%	0%	0%	0%	0%	0%	0%	0%	0%	0%	0%	0%	0%	0%	0%	0%	0%	18%	84%								
12	a	0%	0%	0%	0%	0%	0%	0%	0%	0%	0%	0%	0%	0%	0%	0%	0%	0%	0%	0%	0%	0%	0%	0%	0%							
	b	0%	0%	0%	0%	0%	0%	0%	0%	0%	0%	0%	0%	0%	0%	0%	0%	0%	0%	0%	0%	0%	0%	0%	0%	73%						
13	a	0%	0%	0%	0%	0%	0%	0%	0%	0%	0%	0%	0%	0%	0%	0%	0%	0%	0%	0%	0%	0%	0%	0%	0%	0%	0%					
	b	0%	0%	0%	0%	0%	0%	0%	0%	0%	0%	0%	0%	0%	0%	0%	0%	0%	0%	0%	0%	0%	0%	0%	0%	0%	0%	30%				
14	a	0%	0%	0%	0%	0%	0%	0%	0%	0%	0%	0%	0%	0%	0%	0%	0%	0%	0%	0%	0%	0%	0%	0%	0%	0%	0%	0%	0%			
	b	0%	0%	0%	0%	0%	0%	0%	0%	0%	0%	0%	0%	0%	0%	0%	0%	0%	0%	0%	0%	0%	0%	0%	0%	0%	0%	0%	0%	78%		
15	a	0%	0%	0%	0%	0%	0%	0%	0%	0%	0%	0%	0%	0%	0%	0%	0%	0%	0%	0%	0%	0%	0%	0%	0%	0%	0%	0%	0%	0%	0%	
16	a	0%	0%	0%	0%	0%	0%	0%	0%	0%	0%	0%	0%	0%	0%	0%	0%	0%	0%	0%	0%	0%	0%	0%	0%	0%	0%	0%	0%	0%	0%	0%

6 CONCLUSION

This paper deals with the algorithms for phase calculation in measurement with images methods using the phase shifting technique. It describes several multistep phase shifting algorithms with the constant, but unknown phase step between the captured intensity frames. The new algorithms are shown to be capable of processing the optical signal of Moire images. These techniques are very precise, easy to use, and have a small cost. The results show that new algorithms were precise and accurate. On the basis of the performed error analysis it can be concluded that the new algorithms are very good phase calculation algorithms. These algorithms also seem to be a very accurate and stable phase shifting algorithm with the unknown phase step for a wide range of phase step values. The metric analysis of the considered system

demonstrated that its uncertainties of measurement depend on the frame period of the grid, of the resolution in pixel of photos and of the number of frames. However, the uncertainties of measurement of the geometric parameters and the phase still require attention. In theory, if we have many frames, the measurement errors become very small. The measurement results obtained by the optical system demonstrate its industrial and engineering applications.

Acknowledgements The authors appreciate the generous support of the Pontificia Universidade Catolica de Minas Gerais – PUCMINAS, as well as of the Conselho Nacional de Desenvolvimento Cientifico e Tecnologico – CNPq – "National Counsel of Technological and Scientific Development".

References

[1] R. R. Cordero, J. Molimard, A. Martinez, and F. Labbe. Uncertainty analysis of temporal phase-stepping algorithms for interferometry. *Optics Communications*, 275(1):144–155, 2007.

[2] K. Creath. Phase-measurement interferometry techniques. In E. Wolf, editor, *Progress in Optics*, volume XXVI, page 349, Amsterdam, 1988. Elsevier Science Publishers.

[3] K. Creath. Phase-measurement interferometry techniques. In E. Wolf, editor, *Progress in optics*, volume XXVI, pages 349–393, Amsterdam, 1988. Elsevier Science.

[4] D. C. Ghiglia and M. D. Pritt. *Two-dimensional phase unwrapping: Theory, algorithms and software*. John Wiley & Sons, New York, 1998.

[5] C. Han and B. Han. Error analysis of the phase-shifting technique when applied to shadow moire. *Appl. Opt.*, 45: 1124–1133, 2006.

[6] F. S. Hillier and G. J. Lieberman. *Introduction to operations research*. McGraw-Hill, 8th edition, 2005.

[7] J. M. Huntley. Noise imune phase unwrapping algorithm. *Appl. Opt.*, 28:3268–3270, 1989.

[8] D. Malacara, editor. *Optical shop testing*. John Wiley & Sons, New York, 1992.

[9] D. Malacara, M. Servın, and Z. Malacara. *Interferogram Analysis for Optical Testing*. Taylor & Francis, New York, 2005.

[10] J. Novak. Five-step phase-shifting algorithms with unknown values of phase shift. *International Journal for Light and Electron Optics*, 114(2):63–68, 2003.

[11] J. Novák et al. Multi-step phase-shifting algorithms insensitive to linear phase shift errors. *Optics Communications*, 281(21):5302–5309, 2008. doi:10.1016/j.optcom.2008.07.060.

[12] H. Schreiber and J. H. Bruning. Phase shifting interferometry. In D. Malacara, editor, *Optical Shop Testing*, page 547, New York, 2007. Wiley Interscience.

[13] M. F. Triola. *Elementary Statistics*. Addison Wesley, 10th edition, 2007.

[14] E. Zappa and G. Busca. Comparison of eight unwrapping algorithms applied to fourier-transform profilometry. *Optics and Lasers in Engineering*, 46(2):106–116, 2008.